

The magnetic field topology in the reconnecting pulsar magnetosphere (Research Note)

I. Contopoulos

Research Center for Astronomy, Academy of Athens, 11527 Athens, Greece
e-mail: icontop@academyofathens.gr

Received 25 January 2007 / Accepted 16 April 2007

ABSTRACT

We show that toroidal magnetic field annihilation in the equatorial current sheet of the pulsar magnetosphere is related to how fast poloidal magnetic field lines close as we move away from the light cylinder. This determines the radial reconnection electric field which directly accelerates particles in the neutral layer inside the equatorial current sheet. The efficiency of the poloidal magnetic field closure near the light cylinder may be measurable through the pulsar braking index. We argue that the lower the efficiency of pair formation, the higher the braking index. We also argue that the synchrotron radiation reaction in the neutral layer does not inhibit the accelerated particles from reaching the maximum energy of about $\sim 10^{16}$ eV that is available in the open pulsar magnetosphere.

Key words. stars: pulsars general – magnetic fields – acceleration of particles

1. Introduction

After almost 40 years of pulsar research, the structure of the pulsar magnetosphere, the region extending from the neutron star surface to the wind termination shock, is still not clearly understood. The observed pulsed radiation (radio to gamma ray) is believed to originate in the magnetosphere, and yet it is still not clear where and how it is produced (e.g. Arons 1983; Muslimov & Harding 2004). The magnetosphere is also the source of a fast particle wind with Lorentz factor on the order of 10^6 that terminates in a standing shock at a distance of about 0.1 pc (Bogovalov & Aharonian 2000). Several acceleration mechanisms have been proposed, ranging from ideal MHD models (Contopoulos & Kazanas 2002; Vlahakis 2004), pressure driving (Coroniti 1990; Michel 1994; Kirk & Skjæraasen 2003), to direct particle acceleration in the equatorial current sheet (Romanova et al. 2005; Contopoulos 2007), but we still do not understand how this wind is produced.

In recent years, there has been mounting evidence against ideal MHD wind acceleration, and there is no convincing self-consistent, ideal MHD wind solution available in the literature (Bogovalov 1997). Thus, we decided to direct our attention to models that contain regions where ideal MHD breaks down. The most promising of these regions is the equatorial current sheet, across which the main magnetic field component, the toroidal one, changes direction and annihilates (Contopoulos 2007). Annihilation of the toroidal magnetic field component is associated with an electric field that accelerates particles directly inside the current sheet. Although several authors have acknowledged the presence of this electric field (e.g. Kirk 2004; Romanova et al. 2005), we feel that a certain important physical element has been neglected in the discussion, namely the global topology of the poloidal magnetic field.

In Contopoulos (2007), we dealt with non-ideal MHD regions through the notion of the effective magnetic diffusivity. In

the present work, we give a simpler picture without mentioning the magnetic diffusivity in the equatorial current sheet. In Sect. 2 we argue that toroidal magnetic field annihilation cannot be studied independently of the poloidal magnetic field. In Sect. 3 we associate the pulsar braking index to the rate at which poloidal magnetic-field lines close with distance in the vicinity of the light cylinder. Finally, in Sect. 4 we discuss the issue of particle acceleration in the equatorial current sheet.

2. The global topology of the pulsar magnetosphere

Let us introduce a spherical system of coordinates (r, θ, ϕ) centered on the neutron star and aligned with its axis of rotation. The neutron star rotation delineates two distinct hemispheres, the upper and lower, separated by the rotation equator. The magnetic field also delineates two half spaces: the north, where the magnetic field points away from the star, and the south, where the magnetic field points towards the star. In general, the rotation and magnetic axes are at an angle $\vartheta \neq 0$, and we may assume without any loss of generality that $\vartheta < 90^\circ$. In that case, B_r is mostly positive in the upper (“north”) hemisphere, whereas it is mostly negative in the lower (“south”) hemisphere.

In the case of an isolated pulsar, all magnetospheric field lines naturally originate on the surface of the neutron star, since the source of the magnetospheric field is the neutron star interior. Obviously, solutions also exist with field lines not connected to the star (Lovelace et al. 2006), and these may very well apply to neutron stars surrounded by disks with disk winds, but not to isolated neutron stars. The star holds the magnetic field from diffusing to infinity. The field close to the neutron star is dipolar, but as we move away from the stellar surface, the magnetic field topology is gradually distorted. The magnetic field is stretched outwards and is wound backwards because of the neutron star’s rotation. The distortion depends on the magnetospheric plasma conductivity, on the inclination angle

between the rotation and magnetic axes, and, as we will see, on the neutron star spindown history. The above characteristics can be found in several numerical solutions of simple limiting cases (e.g. Contopoulos et al. 1999; Spitkovsky 2006).

Let us now discuss the significance of the magnetospheric plasma conductivity, first considering the case of infinite plasma conductivity. Ideal MHD requires that plasma is confined to flowing along the magnetic field, so field lines may be visualized as co-rotating with the neutron star at the stellar angular velocity Ω . This does not mean that the magnetospheric plasma co-rotates with the star. The plasma angular velocity is equal to Ω only wherever $B_\phi = 0$ (e.g. Beskin 1997). A direct corollary of this is that no field lines close outside the light cylinder, which is the cylindrical distance $r_L \equiv c/\Omega$, where if a particle were to corotate with the neutron star, it would do so at the speed of light. The argument is straightforward: as we said, field lines from both stellar magnetic hemispheres are wound backwards by the neutron star's rotation; therefore, a point on every closed field line may be found where $B_\phi = 0$. If a closed field line were to extend beyond the light cylinder, that point would lie outside the light cylinder, and according to our discussion above, the plasma velocity there would have to be at least equal to $r\Omega \sin\theta > c$. The unavoidable conclusion is that the pulsar magnetosphere consists of closed field lines that corotate with the neutron star inside the light cylinder and of field lines that cross the light cylinder and open up to infinity. It is important to keep in mind that nothing exceptional takes place at the light cylinder, because field lines cross it without kinks or discontinuities (Contopoulos et al. 1999). Several authors have shown that asymptotically ($r \gtrsim r_L$), the poloidal magnetic field structure becomes radial (monopole-like). In the axisymmetric case ($\theta \approx 0$), the open poloidal magnetic flux in each magnetic hemisphere is given by

$$\Psi(r, \theta) \approx \Psi_L(1 - \cos\theta), \quad (1)$$

and the magnetic field by

$$|B_r(r, \theta)| \approx B_L \left(\frac{r}{r_L}\right)^{-2}, \quad B_\theta(r, \theta) \approx 0 \text{ and}$$

$$|B_\phi(r, \theta)| \approx B_L \sin\theta \left(\frac{r}{r_L}\right)^{-1} \quad (2)$$

(Michel 1994; Contopoulos et al. 1999). Here, $B_L \equiv \Psi_L/(2\pi r_L^2)$ is a typical value for the magnetic field at about the light cylinder distance. As Bogovalov (1999) shows in a very important and elegant paper, Eqs. (2) are valid even in the case of an oblique (i.e. non-aligned) magnetic rotator. In that case, in the upper hemisphere, magnetic field lines mostly point away from the star ($B_r > 0$, $B_\phi < 0$), whereas in the lower hemisphere they mostly point towards it ($B_r < 0$, $B_\phi > 0$). The two regions are separated by a spiral current-sheet discontinuity described by Eq. (3) in Kirk & Lyubarski (2001), across which B_r and B_ϕ change sign together.

Let us next consider the more realistic case of high, but not infinite, plasma conductivity. It is natural to argue that ideal MHD is a realistic description of the largest part of the pulsar magnetosphere, except for restricted regions with high electric-current densities, where ideal MHD breaks down (Contopoulos 2007). In that case, field lines are not forbidden to close outside the light cylinder. In fact, several numerical solutions that try to simulate the ideal MHD magnetosphere show this different topology because of numerical diffusivity (Komissarov 2006; McKinney 2006; Spitkovsky 2006). It is

very important to note that field-line closure outside the light cylinder may take place only if it is associated with magnetic field energy dissipation (non-ideal MHD). In fact, several authors have proposed that this mechanism may be related to the acceleration of the pulsar wind, and this led to the so-called ‘‘striped’’ pulsar wind model (Coroniti 1990; Michel 1994; Lyubarsky & Kirk 2001; Kirk & Skjæraasen 2003).

There is here, we believe, a subtle but very important point that has been overlooked by most previous studies of magnetic field dissipation in the current sheet outside the light cylinder, and this has to do with the global topology of the reconnecting magnetic field. Equations (2) imply that, next to the region of reconnection in the striped wind at large distances ($r \gg r_L$), it is the toroidal magnetic field component that is the dominant one. Several authors, therefore, opted to ignore the poloidal magnetic field component altogether and instead study reconnection as if it were taking place exclusively in the toroidal magnetic field component. It is as if the star ‘‘shoots out’’ rings of a toroidal magnetic field with different ϕ -direction depending on whether they originate in the north or south magnetic hemispheres. The problem with that approach is that, by ignoring the global topology of the poloidal magnetic field component, we miss the crucial fact that the source of the toroidal magnetic field component is the azimuthal winding of the poloidal one.

This is not without significance. All field lines originate on the surface of the star, and there is a finite amount of magnetic flux that crosses the light cylinder and would be stretched out to infinity, were it not for the presence of equatorial current sheet reconnection. Obviously, as toroidal magnetic field annihilation proceeds, less and less poloidal magnetic flux extends to larger distances¹. As a result, less and less open field lines are available for reconnection or for carrying with them the stellar spindown energy in the form of Poynting flux. We may thus generalize Eqs. (1) and (2) and introduce a simple power law scaling

$$\Psi(r, \theta) \approx \Psi_L(1 - \cos\theta) \left(\frac{r}{r_L}\right)^{-\epsilon}, \quad (3)$$

where $\epsilon \ll 1$ is a small positive parameter that obviously depends on the (yet unknown) physics of gradual reconnection in the equatorial sheet. At this stage, we can only take it to be a free parameter. Equation (3) is an ad hoc generalization of Eq. (1), and is not based on current theory or observations. It may, however, be valid as a toy model that describes toroidal magnetic field annihilation and poloidal magnetic field reconnection in the vicinity of the light cylinder. Obviously, in order to study how fast toroidal magnetic field annihilation proceeds with distance, one needs to solve a formidable non-force-free (beyond the fast magnetosonic surface) relativistic MHD problem that incorporates the microphysics of field annihilation. It is interesting to note that recent time-dependent numerical simulations (Bucciantini et al. 2006) suggest that reconnection may be sporadic, spontaneous, and limited in the vicinity of the closed line zone.

Having acknowledged the limitations of our toy model, it is now straightforward to show that

$$|B_r(r, \theta)| \approx B_L \left(\frac{r}{r_L}\right)^{-2-\epsilon}, \quad B_\theta(r, \theta) \approx \epsilon B_L \left(\frac{r}{r_L}\right)^{-2-\epsilon} \text{ and}$$

$$|B_\phi(r, \theta)| \sim B_L \sin\theta \left(\frac{r}{r_L}\right)^{-1-\epsilon}. \quad (4)$$

¹ In other words, toroidal magnetic field annihilation proceeds in the north-south direction.

Note that B_θ is everywhere of the same sign. This component of the magnetic field, which up to now has been considered insignificant, may have interesting observable implications. In fact, Petri & Kirk (2005) present a plausible physical model for the Crab pulsar, where high energy radiation originates in the equatorial current sheet at a distance of about $10r_L$. In their model, they require a magnetic field component B_θ roughly 10% of B_ϕ , which is not very different from what Eqs. (4) yield for $\epsilon \lesssim 1$.

We conclude this section by emphasizing that annihilation of the toroidal magnetic field in the equatorial current sheet may be studied only in conjunction with studying the poloidal structure of the magnetospheric field. To our knowledge, this has not been taken into account in any existing model of extended equatorial field annihilation (e.g. Lyubarsky & Kirk 2001; Romanova et al. 2005).

3. Evolution of the pulsar magnetosphere with neutron star spindown

As we argued in Contopoulos (2007), the rate of equatorial current-sheet reconnection in the vicinity of the light cylinder may be indirectly measurable through observations of the neutron star's braking index

$$n \equiv \frac{\delta \ln \dot{\Omega}}{\delta \ln \Omega}. \quad (5)$$

In that work, we dealt with non-ideal MHD regions through the notion of the effective magnetic diffusivity. In the present work, we give a simpler picture without mentioning the magnetic diffusivity in the equatorial current sheet.

In the above picture of finite plasma conductivity, magnetic field lines enter the equatorial current sheet at a grazing angle, i.e. $|B_r| \gg B_\theta$ outside the current sheet. Electromagnetic energy is continuously “pumped” into it and is lost in accelerating particles in the current sheet (see next section). In other words, equatorial toroidal magnetic field annihilation prevents poloidal magnetic flux from reaching “infinite” distances. The picture we describe here may even be thought to take place in steady state were it not for the fact that the neutron star actually spins down.

Why is the neutron star spindown so important? We remind the reader that, inside the light cylinder, the pulsar magnetosphere consists of a co-rotating region of closed field lines and of a certain amount Ψ_{open} of open poloidal magnetic flux which extends beyond the light cylinder. It is well known that the spindown rate $\dot{\Omega}$ depends on Ω and Ψ_{open} as

$$\dot{\Omega} \propto \Omega \Psi_{\text{open}}^2 \quad (6)$$

(Contopoulos 2005). Let us backtrack for a moment and assume that reconnection does not take place anywhere in the pulsar magnetosphere. In that case, as the neutron star spins down, the light cylinder moves out at a certain rate (roughly 1 km per year), but the region of closed field lines cannot grow, since the absence of reconnection prevents open field lines from closing and accumulating on top of the closed line region, and thus Eq. (1) implies that $\Psi_{\text{open}} \equiv \Psi_L = \text{const}$. According to Eqs. (5) and (6), the neutron star braking index would be measured to be equal to 1, which is not what is observed. Now let us once again consider the physically more interesting case where reconnection does take place in the vicinity of the light cylinder, only it is confined inside the equatorial current sheet. In that case, as the neutron star spins down and the light cylinder moves out, it encompasses more and more poloidal magnetic flux because, as we

argued, in the vicinity of the light cylinder magnetic flux closes with distance at a rate given by Eq. (3). When the light cylinder moves out from r_L to $r_L + \delta r_L$, a certain amount of poloidal magnetic flux,

$$\delta \Psi_{\text{open}} \approx -\epsilon \Psi_L \left(\frac{\delta r_L}{r_L} \right) = \epsilon \Psi_L \left(\frac{\delta \Omega}{\Omega} \right), \quad (7)$$

is now found contained inside the new light cylinder. Under ideal MHD conditions, however, the stellar spindown energy is transferred only along field lines that cross the light cylinder²; therefore, our result in Eq. (7) modifies the neutron star spindown rate by an amount

$$\delta \dot{\Omega} = (1 + 2\epsilon) \frac{\dot{\Omega}}{\Omega} \delta \Omega, \quad (8)$$

which yields a braking index value of

$$n = 1 + 2\epsilon. \quad (9)$$

The reader may have noticed that our present discussion differs from the one in Contopoulos (2007), where we introduced an effective magnetic diffusivity η , which is responsible for both the equatorial reconnection of the toroidal magnetic field and the inward diffusion of the poloidal magnetic field lines. In the present work, we again consider magnetic field energy losses in the equatorial current sheet, but we also argue that the growth of the closed-line region is directly related to the advancement of the light cylinder to larger distances as the neutron star spins down.

We repeat once again that toroidal magnetic field annihilation is related to how fast poloidal magnetic field lines reconnect as we move away from the light cylinder (Eqs. (3) and (4)). This is very important, because the efficiency of poloidal magnetic field closure is something that may be measurable through the pulsar braking index, and thus yield an estimate of the physical processes that lead to magnetic field reconnection in the pulsar magnetosphere.

4. Particle acceleration in the equatorial current sheet

Equations (4) are valid outside the current sheet discontinuity. Inside the sheet, B_r and B_θ change sign, meaning a neutral layer develops where the only remaining magnetic field component is B_θ . In other words, when we generalize Bogovalov (1999), reconnection may take place at various positions along the current sheet discontinuity. All field lines originate on the surface of the star; therefore, as we argued, they carry with them the information that the neutron star is rotating at angular velocity Ω throughout the region where ideal MHD is a valid physical approximation. In axisymmetry, a poloidal electric field develops perpendicular to the poloidal magnetic field because of the neutron star rotation, with magnitude

$$E = \frac{r\Omega \sin \theta}{c} (B_r^2 + B_\theta^2)^{1/2} \quad (10)$$

² As we show in the next section, a radial electric field equal to $E_r = B_\theta(r/r_L)$ appears inside the equatorial current sheet. Obviously, inside the light cylinder, $\mathbf{E} \perp \mathbf{B}$ and $E_r < B$, so electromagnetic field energy cannot be dissipated through direct particle acceleration in the equatorial current sheet.

(e.g. Beskin 1997). Magnetic flux surfaces are, therefore, isopotential surfaces, with potential difference between them given by

$$\delta V = \frac{\Omega}{2\pi c} \delta \Psi, \quad (11)$$

where $\delta \Psi$ is the magnetic flux contained between the two flux surfaces. This is valid along each field line, all the way from its footpoint on the stellar surface to the point where that field line reaches the equatorial current sheet and reconnects (if that particular one does) with the corresponding field line from the opposite magnetic hemisphere. According to our discussion above, this implies that the magnetospheric potential drop manifests itself along the equatorial sheet wherever poloidal field lines reconnect. Another way to understand this is that, wherever reconnection takes place, a radial electric field equal to

$$E_r = \frac{r \sin \theta}{r_L} B_\theta \quad (12)$$

develops in the interior of the current sheet where $B_r \sim B_\phi \sim 0$. This is the reconnection electric field component mentioned in Kirk (2004) and Romanova et al. (2005) that accelerates particles in the current sheet. The new result in our present work is that E_r is directly proportional to $B_\theta \neq 0$ in the current sheet.

As long as a particle stays in the interior of a reconnection region in the equatorial current sheet, it will be accelerated to an energy equal to $e\delta V$, where e is the electron charge, and δV is the potential drop associated with the poloidal field lines at the two ends of the acceleration region. Current sheets are known to be unstable, so we expect that the pulsar equatorial current sheet will also be fragmented into several short acceleration regions. Nevertheless, one may argue that some particles may manage to profit from several of these acceleration regions. In such a stochastic acceleration, some particles may manage to get accelerated to the maximum energy available in the open pulsar magnetosphere, i.e. to the energy due to the potential drop across field lines that originate on the magnetic pole and the edge of the neutron star polar cap, namely $\sim 10^{16}$ eV (De Jager & Harding 1992).

We argue that synchrotron radiation reaction does not inhibit the acceleration. We performed a straightforward calculation of relativistic electron/positron orbits as they enter the current sheet (Figs. 1 and 2) and realized that their orbit becomes more and more confined around the center of the current sheet where $B_r \sim B_\phi \sim 0$. Therefore, even if one is willing to keep our toy model scaling all the way from r_L to $r \gg r_L$, the synchrotron radiation reaction due to the B_θ component of the magnetic field will limit the acceleration only when the particles reach a Lorentz factor on the order of

$$\Gamma_{\max} \sim 10^8 \left(\frac{r}{r_L} \right)^{1/2} B_L^{-1/2} \gg 10^8, \quad (13)$$

where, B_L is measured in Gauss. Thus, synchrotron radiation is unimportant inside the pulsar wind termination shock.

We end our discussion with an order-of-magnitude estimate of the acceleration length l_{acc} in the vicinity of the light cylinder. Electromagnetic energy flux enters the current sheet from above and below at a rate of $2(E_r B_\phi / 4\pi c)(B_\theta / B_r)$. This is absorbed by the particle flux $2\kappa n_{GJ} c (B_\theta / B_r)$, which also enters the current sheet from above and below. Here, $\kappa \sim 10^3 - 10^5$ is the multiplicity of pair production in magnetospheric gaps (Daugherty & Harding 1982; Gurevich & Istomin 1985), and $n_{GJ} \sim \Omega B_r / (4\pi c e)$ is the Goldreich-Julian number density (Goldreich & Julian 1969). If we assume an acceleration length

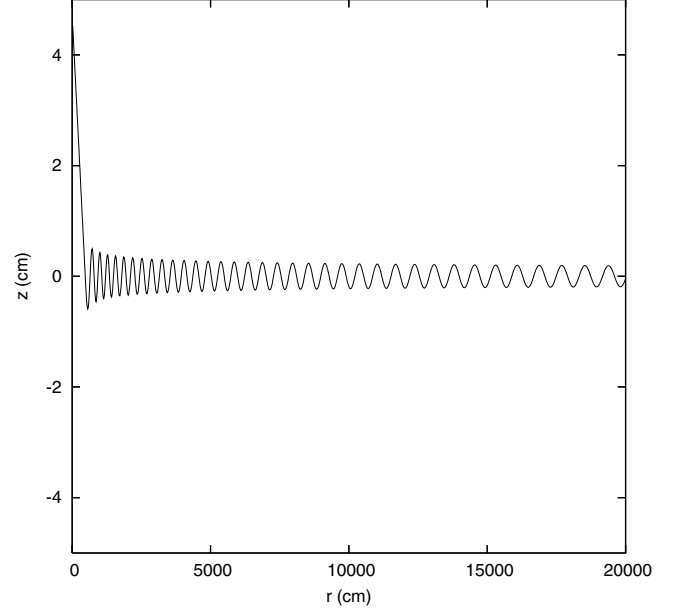


Fig. 1. Calculated electron orbits that enter the equatorial current sheet $z = 0$ from above. The units are in centimeters. We consider only the axisymmetric case $\vartheta = 0$. The injection region is at $r = 10r_L$. Here, $B_\theta / B_r = 10^2$ on the surface of the current sheet. We took $r_L = 1500$ km and $B_L = 10^6$ G (values representative of the Crab pulsar). Initially, the relativistic electrons move together with the magnetic field with Lorentz factor equal to ~ 100 . The Lorentz factor grows linearly with the acceleration distance. We observe that the particles do not escape from the current sheet (unless of course the current sheet is terminated), and are confined more and more around the center of the current sheet where $\mathbf{B} = B_\theta \hat{\theta}$.

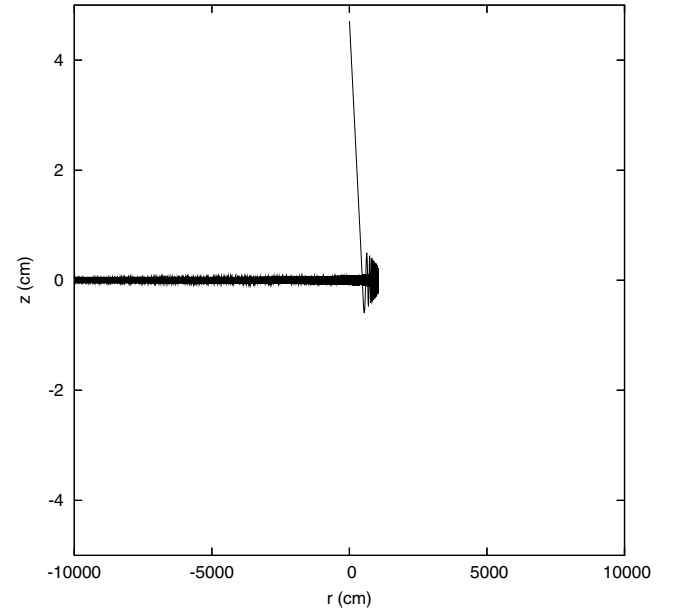


Fig. 2. Same as Fig. 1 for positrons.

$l_{\text{acc}} \ll r$, a straightforward energy balance in the current sheet yields

$$l_{\text{acc}} \sim \frac{r}{2\kappa\epsilon}. \quad (14)$$

A (typical) value of ϵ on the order of one half yields $l_{\text{acc}} \sim 10^{-4} r \ll r$. On the other hand, if we know l_{acc} from a numerical simulation of the pulsar current sheet fragmentation (e.g. Crew et al. 2001; Bessho & Bhattacharjee 2005), Eq. (14) yields

ϵ , which determines the global topology of the pulsar magnetosphere for various values of the multiplicity parameter κ . We thus predict that the smaller the efficiency of pair production, the larger ϵ is. Unfortunately, the 6 pulsars with the best-measured values of the braking index are all strong pair creators, and therefore, our prediction cannot be tested observationally using only those particular 6 pulsars.

5. Summary

In the present work, we argue that toroidal magnetic field annihilation in the equatorial current sheet of the pulsar magnetosphere cannot be studied independently of the poloidal magnetic field. This association allows us to relate the pulsar braking index to the rate at which poloidal magnetic field lines close with distance in the vicinity of the light cylinder. This also allows us to estimate the reconnection electric field that develops in the interior of the equatorial current sheet. We show that this electric field accelerates electrons and positron in opposite directions, and we predict that there will be little or no synchrotron radiation in the region upstream of the wind termination shock. In fact, some particles may even profit from the full potential drop in the open line region and thus reach energies on the order of 10^{16} eV. Finally, we associate the efficiency of equatorial reconnection to the efficiency of pair production in the pulsar magnetosphere.

Acknowledgements. We would like to thank Pr. Roger Blandford for his hospitality at the Kavli Institute for Particle Astrophysics and Cosmology in July 2006 when most of the ideas in the present work originated.

References

- Arons, J. 1983, *ApJ*, 266, 215
Beskin, V. S. 1997, *Physics-Uspekhi*, 40, 659
Bessho, N. & Bhattacharjee, A. 2005, *Phys. Rev. Lett.*, 95, 245001
Bogovalov, S. V. 1997, *A&A*, 327, 662
Bogovalov, S. V. 1999, *A&A*, 349, 1017
Bogovalov, S. V. & Aharonian, F. A. 2000, *MNRAS*, 313, 504
Bucciantini, N., Thompson, T. A., Arons, J., Quataert, E. & Del Zanna, L. 2006, *MNRAS*, 368, 1717
Contopoulos, I. 2006, *A&A*, 442, 579
Contopoulos, I. 2007, *A&A*, 466, 301
Contopoulos, I. & Kazanas, D. 2002, *ApJ*, 566, 336
Contopoulos, I., Kazanas, D. & Fendt, C. 1999, *ApJ*, 511, 351
Coroniti, F. V. 1990, *ApJ*, 349, 538
Crew, S., Nishikawa, K.-I., Büchner, J. & Kotzé, P. B. 2001, *Proc. ISSS-6*, 1
Daugherty, J. K. & Harding, A. K. 1982, *ApJ*, 252, 337
De Jager, O. C. & Harding, A. K. 1992, *ApJ*, 396, 161
Goldreich, P. & Julian, W. H. 1969, *ApJ*, 157, 869
Gurevich, A. V. & Istomin, Ia. N. 1985, *ZhETF*, 89, 3
Kirk, J. G. 2004, *Lprl*, 92, 181101
Kirk, J. G. & Lyubarsky, Y. 2001, *PASA*, 18, 415
Kirk, J. G. & Skjæraasen, O. 2003, *ApJ*, 591, 366
Komissarov, S. S. 2006, *MNRAS*, 367, 19
Lovelace, R. V. E., Turner, L. & Romanova, M. M. 2006, *ApJ*, 652, 1494
Lyubarsky, Y. & Kirk, J. G. 2001, *ApJ*, 547, 437
McKinney, J. C. 2006, *MNRAS*, 368, L30
Michel, F. C. 1994, *ApJ*, 431, 397
Muslimov, A. G. & Harding, A. K. 2004, *ApJ*, 606, 1143
Petri, J. & Kirk, J. G. 2005, *ApJ*, 627, L37
Romanova, M. M., Chulsky, G. A. & Lovelace, R. V. E. 2005, *ApJ*, 630, 1020
Spitkovsky, A. 2006, *ApJ*, 648, L51
Vlahakis, N. 2004, *ApJ*, 600, 324